

Possible stress-induced phase transition in *o*-TaS₃

Kanta Das, M. Chung, M. J. Skove, and G. X. Tessema

Department of Physics and Astronomy, Clemson University, Clemson, South Carolina 29634

(Received 12 April 1995)

We have measured the stress-strain (σ - ϵ) relations in *o*-TaS₃ below the charge-density-wave (CDW) transition temperature. We find a large peak in $d\epsilon/d\sigma$ at a critical stress $\sigma_c \approx 0.7$ GPa below 200 K. The anomaly in $d\epsilon/d\sigma$, as large as 50% and perhaps associated with a change in length, is sample and temperature dependent. We show that this anomaly is associated with previously seen anomalies in the elastic and transport properties of TaS₃, and propose that there is a weakly first-order phase transition from one CDW phase to a different CDW phase at σ_c .

The orthorhombic form of the transition-metal trichalcogenide *o*-TaS₃ is one of the most extensively studied charge-density-wave (CDW) materials.^{1,2} It undergoes a Peierls transition at $T_p = 220$ K. The electrical conductivity at low applied electric field E shows a semiconducting behavior below T_p . When an electric field greater than a threshold field E_t is applied, the CDW becomes depinned, leading to non-Ohmic conductivity and a narrow band noise (NBN), whose frequency is related to the velocity of the CDW.¹ There is an anomaly in Young's modulus Y at T_p .³ Below T_p , the Y and the shear modulus G of TaS₃ are dependent on E , decreasing by as much as 2 and 20%, respectively, for $E \gg E_t$.^{4,5} Moreover, these anomalies have been observed to depend on the measured frequency.^{6,7} The CDW in *o*-TaS₃ is slightly incommensurate with the underlying lattice⁸ with a wave vector $\mathbf{q} = \frac{1}{2}\mathbf{a}^* + \frac{1}{8}\mathbf{b}^* + 0.225\mathbf{c}^*$ near T_p , where \mathbf{a}^* , \mathbf{b}^* , and \mathbf{c}^* are the reciprocal lattice vectors of the underlying lattice. It has been shown by electron-diffraction studies that there is a tendency toward commensurability as the temperature is lowered, perhaps leading to fourfold commensurability near 140 K.⁹

It is by now well known that *o*-TaS₃ has very unusual changes in its transport¹⁰⁻¹⁵ and elastic¹⁵ properties when stress σ is applied along the chain direction (c -axis). The conductivity at low electric field, due to the normal carriers, increases with σ and has a maximum at the critical stress σ_c , while the high field conductivity, i.e., at $E \gg E_t$, has a minimum at σ_c . Two threshold fields were observed for $\sigma \approx \sigma_c$. At larger σ , the first or higher threshold field E_{t1} disappears and only a second or lower threshold field E_{t2} survives. Interestingly, the NBN vanishes near σ_c ,^{11,14,15} motivating the suggestion that the CDW becomes commensurate, which is consistent with the local minimum in the conductivity at $E \gg E_t$ near σ_c , particularly at low T . The NBN reappears at larger σ , where the CDW is presumably again incommensurate, with a sharper and larger amplitude than at small σ . It was also observed that the anomaly in G , i.e., $[G(E=0) - G(E \gg E_t)]/G(E=0)$, is greatly reduced for $\sigma > \sigma_c$.¹⁵

Although several models were put forth to explain the unusual strain (ϵ) dependence of the properties of TaS₃,

to date none of them are completely successful. In this paper, we report on measurements of σ versus strain ϵ and $d\epsilon/d\sigma$ versus σ for *o*-TaS₃. We find a large peak in $d\epsilon/d\sigma$, which may be due to a change in the length of the sample L , at $\sigma_c \approx 0.7$ GPa below 200 K, both of which are sample and temperature dependent. The observed anomalies in $d\epsilon/d\sigma$ and L at σ_c , associated with the appearance of two threshold fields, are correlated with the stress dependence of the transport properties of TaS₃.

Single crystals of TaS₃ were grown by the standard vapor transport technique described elsewhere.^{2,14} The size of crystals used in this work was typically 3 mm \times 7 μ m \times 2 μ m, where the thickness of the sample was estimated from the room-temperature resistance (520 Ω) and resistivity of *o*-TaS₃ ($= 3 \times 10^{-6}$ Ω m).^{1,2} E_t 's were typically 16 V/m at 120 K for our unstrained samples.

The sample was mounted on a stress-strain device, which has been described elsewhere in detail.^{16,17} One end of the sample was attached to a movable metal plate and the other end glued to a fixed plate. The strain was measured using parallel capacitor plates with one plate attached to the main body of the device and the other plate moving with the movable end of the sample. On each metal plate, there are two copper wires allowing electrical contacts (four probe) to be made to the sample. Silver paint was used to make electrical contacts between the sample and the copper wires. To prevent the sample from slipping through the contacts while pulling, epoxy was placed over the sample between the contacts.

To apply a force on the sample, two magnets fixed on the metal rod apply a force to the rod proportional to the current in a solenoid, which surrounds the two magnets. The rod is supported by two leaf springs, which apply a small restoring force to the rod. The force applied by the magnets F_M is calculated from the coil current, which in turn is calibrated by hanging weights. The small force F_X applied to the rod by the springs that hold the rod is subtracted to find the force F_S ($= F_M - F_X$) on the sample. The relation between the position of the rod and capacitance was calibrated using a microscope. $\sigma = F_S/A$ and $\epsilon = \Delta L/L$ in the sample can then be calculated, where A is the cross section and ΔL the change in length of the

sample. Y is given by $d\sigma/d\varepsilon|_{\varepsilon=0}$. $d\varepsilon/d\sigma$ was measured directly using what we refer to as the two lock-in amplifier technique. Lock-in amplifier No. 1 was used to excite and measure the offset voltage of a capacitance bridge, measuring ΔL , at a frequency of about 2 kHz. A small 28-Hz current from lock-in amplifier No. 2 is superimposed on the dc current in the solenoid of the stress-strain device. The output from lock-in amplifier No. 1 is then fed to the input of lock-in amplifier No. 2, which thus measures the 28 Hz oscillating ε caused by the 28 Hz oscillating σ . The signal measured by lock-in No. 2 is proportional to the derivative of ε with respect to σ , and thus to $1/Y$. Note that the stress σ_{33} in the sample is uniaxial and uniform over the sample except for a small region near the contacts. The strain ε_{33} is measured, but the other ε 's in the sample must be inferred from the elastic constants.

Figure 1 shows the resistance R as a function of σ for several currents at $T=121$ K. This result is typical of the results for the temperature range we studied and as also reported earlier,^{10,14} except the local maximum in R at σ_c at high current is not observed at temperatures above 130 K, for currents up to $100 \mu\text{A}$. We also note that the low and high current R is very asymmetric about σ_c (so is the thermoelectric power^{12,14}).

Figure 2(a) shows $d\varepsilon/d\sigma$ as a function of σ at $T=121$ K. We observe a large peak in $d\varepsilon/d\sigma$ at σ_c , e.g., $\Delta(d\varepsilon/d\sigma)/(d\varepsilon/d\sigma)_0 \approx 20\%$, where $(d\varepsilon/d\sigma)_0$ is the value at σ_c when $d\varepsilon/d\sigma$ is extrapolated from $\sigma < \sigma_c$. The size of the peak and the position value of σ_c are independent of the current applied to the sample, but are dependent on the sample and temperature. This is shown in Figs. 3 and 4 for two samples. We doubled and halved the amplitude of the σ oscillation and saw no change in the size of the anomaly. The anomaly increases with decreasing temperature down to about 100 K, where it is as large as 50% (see Fig. 3). This anomaly is not seen above ~ 200 K. σ_c decreases about 25% from ~ 200 to 100 K and then remains constant down to 85 K (see Fig. 4), as

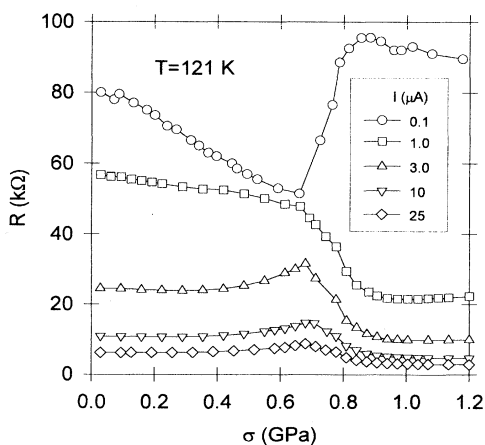


FIG. 1. R vs σ for several current at $T=121$ K. The threshold current at all σ 's was greater than $0.1 \mu\text{A}$. The solid lines are guides to the eye.

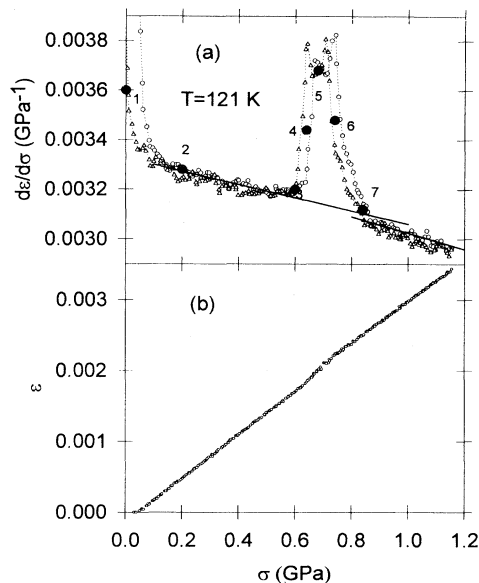


FIG. 2. (a) $d\varepsilon/d\sigma$ vs σ for $I=1.0 \mu\text{A}$. The open circles and triangles are taken with increasing and decreasing σ , respectively. Solid circles with numbers correspond to the σ 's at which the voltage dependence of R was measured as shown in Fig. 5. The solid lines are least square fits to data with increasing σ before and after σ_c . The behavior near $\sigma=0$ is due to the instrument springs as the sample bows. The dotted lines through data points are guides to the eye. (b) ε vs σ curve. Note that this curve is obtained independently of curve (a). The change in curvature in the ε vs σ at σ_c , corresponding to the large anomaly in $d\varepsilon/d\sigma$, may be associated with a length change at σ_c .

also observed in Ref. 10. We note here that ε_c found in this work is about 2–3 times smaller than that of previous studies.^{10–15} The reason may be that ε_c is very sample dependent.

Figure 2(a) also shows a slight hysteresis of 0.03 GPa in σ_c between increasing and decreasing σ . This is prob-

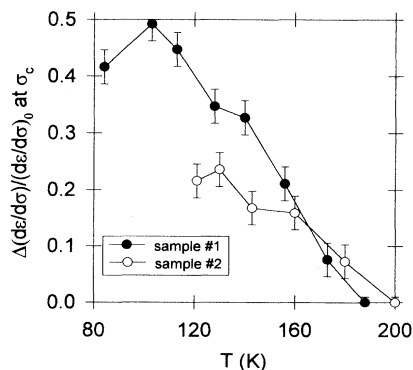


FIG. 3. The normalized height of the anomaly in $d\varepsilon/d\sigma$ at σ_c (for example, the height from the solid line to circle No. 5 in Fig. 2) as a function of temperature for two samples. $(d\varepsilon/d\sigma)_0$ is the value at σ_c when $d\varepsilon/d\sigma$ is extrapolated from $\sigma < \sigma_c$. Data for sample No. 2 were taken only down to 120 K.

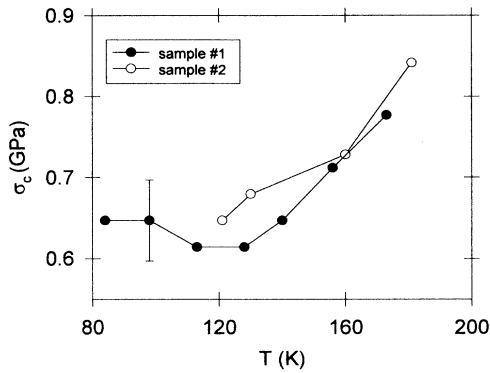


FIG. 4. σ_c vs T for two samples. σ_c is the value of σ at the maximum of the peak in $d\varepsilon/d\sigma$, as in Fig. 2(a). The error bar applies to all the data.

ably due to the intrinsic hysteresis of the apparatus and not inherent to the sample. The anomaly in $d\varepsilon/d\sigma$ at σ_c appears to have double peaks in this sample, but for other samples we studied, it had a flat or sometimes a sharp single peak depending upon sample and temperature. Note that Y and $dY/d\sigma$ are enhanced upon passing through σ_c , shown as solid lines in Fig. 2(a). In models of bulk CDW motion,¹ it has been supposed that a commensurate CDW (CCDW) interacts more strongly with the lattice than an incommensurate CDW (ICDW). If the CDW became commensurate at σ_c , one might expect a slight enhancement of Y . This is consistent with the local maximum in R at high field and the maximum in E_t , all of which would be expected if the CDW became commensurate with the lattice at σ_c .

It is also important to mention the electric field dependence of the change in Y when E is increased beyond E_t at low frequency. In vibrating reed experiments, Y decreases when E exceeds E_t . The decrease is frequency dependent with a maximum of about 2% at 100 Hz. Previous experiments using uniform σ at nearly zero frequency^{17,18} found no change in Y when E exceeded E_t . We attempted to find out if this discrepancy was due to the frequency difference of the experiment or the difference in the σ distribution in the sample (uniform in these experiments and nonuniform in the vibrating reed experiments). Within our experimental error (our resolution is about 1%), we do not observe any change in Y for $E > 10E_t$, consistent with the result of static measurements.^{17,18} The anomaly observed in vibrating reed experiments, measured at 48 Hz at $E \approx 4E_t$,⁷ was smaller than our uncertainty, but extrapolated to $10E_t$, the anomaly seen in vibrating reed experiments would be 1.5%, which, if present in our uniform uniaxial stress experiments at 28 Hz, would have been observed. The difference is, however, too small to say definitely that there is an inconsistency between the two experiments.

In Fig. 2(b), we plot ε versus σ at $T = 121$ K. Near σ_c , there is a finite change in ε with a nearly infinitesimal change in σ . This indicates that the sample has a finite

expansion with an infinitesimal change in σ at σ_c , mimicking the behavior of a first-order phase transition. The region in which there is an anomaly would then be a two-phase region, in which two different phases could coexist in the sample. Application of a small additional force by the magnets would move the boundary between the two phases, rather than changing σ in either phase, as long as the sample were in the two-phase region. Note that the sample can lengthen at constant σ as the magnets apply force and the supporting springs oppose them. Davis *et al.*¹⁴ also associated the large amplitude change and hysteretic behavior in the NBN spectrum with a first-order phase transition at σ_c . The apparent peak in $d\varepsilon/d\sigma$ may be due to this small length change at σ_c rather than to actual changes in Y . The two would be difficult to distinguish with our method.

Figure 5 shows the voltage dependence of R for several σ 's at $T = 121$ K. The stress during this measurement was set to be at the values given by 1–7 in Fig. 2(a). In this way, we can directly compare R data (or E_t data) with $d\varepsilon/d\sigma$ (or Y) data. As seen in Fig. 2, two threshold voltages are unambiguously observed at $\sigma = 0.64$ and 0.68 GPa (shown as the dotted lines), which correspond to the rising region of the peak in $d\varepsilon/d\sigma$ versus σ curve. This is consistent with the presence of two different CDW phases in this region.

In Fig. 6, we show E_t as a function of σ for two temperatures, 121 and 181 K, obtained from Fig. 5. For $T = 121$ K, E_{t1} increases with σ and above σ_c , E_{t2} is nearly independent of σ , whereas for $T = 181$ K, E_{t1} decreases with σ below σ_c . The second and smaller threshold E_{t2} at higher σ is about $0.1E_{t1}$ at lower σ .

The anomalies at σ_c in the transport properties might be attributed to (1) a transition with increasing σ from CDW motion to discommensuration (DC) motion,¹⁰ (2) a transition from an ICDW to a CCDW with no DC

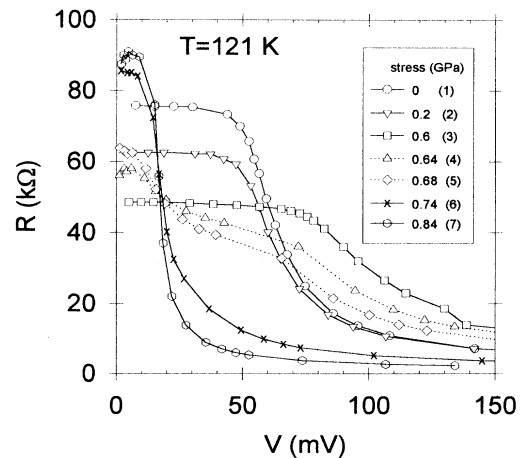


FIG. 5. R vs voltage curve measured at several σ 's denoted by the numbers in Fig. 2(a). Two threshold voltages are observed in the stress region where $d\varepsilon/d\sigma$ increases sharply. The solid and dotted lines are guides to the eye.

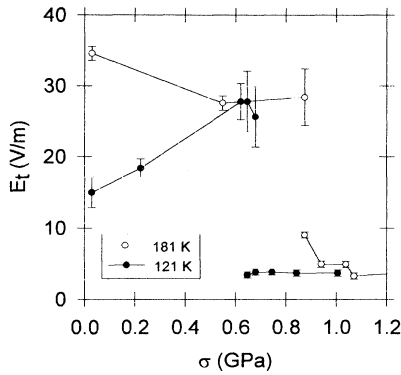


FIG. 6. E_t vs σ at $T=181$ and 121 K. E_t 's were estimated from the R vs voltage curves; the length between potential leads was 2.34 mm. The discontinuity in E_t occurs at σ_c . The lines are guides to the eye.

motion,^{19,20} or (3) a transition between two different CDW phases. We now consider how each fits the experimental data.

Model (1) assumes the non-Ohmic conductivity near σ_c in TaS_3 to be due to the motion of an array of charged DC's (or solitons). The density of DC's decreases to zero as σ approaches σ_c , where the CDW becomes fourfold commensurate. Although a transition between CDW motion and DC motion at σ_c fits much of the experimental transport data, as discussed in Ref. 14, it is difficult to see how this would lead to a transition that is weakly first order, as seen in this work, to an order of magnitude change in $\Delta G/G$, as seen by Xu and Brill¹⁵ or to the asymmetry about σ_c in the resistance anomaly. Further, Wang *et al.*⁹ found from x rays that the CDW becomes commensurate at about 140 K, where no special change in these anomalies occurs. The anomalies we see are present above and below 140 K, in contrast to the argument that the anomaly is due to a transition from an ICDW to a CCDW. Thus, this model is not very likely.

A transition between two phases, one incommensurate and one commensurate, might lead to a weakly first-order transition. According to McMillan,¹⁹ as the transition is approached, DC's appear. The transition from ICDW to CCDW can be thought of as a defect melting transition, with the density of DC's decreasing to zero as the phase boundary is approached. Phase fluctuations provide a repulsive interaction between DC's and amplitude fluctuations an attractive interaction, the sum of which produces a weakly first-order transition. Fisher and Fisher²⁰ find a continuous transition for CCDW to ICDW, with logarithmic divergency in three dimensions. The presence of defects will affect these theories in a way that is hard to predict, and the width of a continuous transition is hard to calculate from first principles. Thus, whether the weakly first-order transition that we observe could be an incommensurate to commensurate transition is not determined by the order of the transition. The transport measurements seem to imply that the high σ phase cannot be commensurate, as there is a lower E_t in the high σ

phase, implying easy motion of the CDW (or DC's), contrary to the usual belief that commensurability pinning would be large. The jump in the thermopower at ϵ_c is consistent with a phase change at ϵ_c .^{12,14} The x-ray results of Wang *et al.*⁹ also seem to rule out such a transition, since nothing happens to the transition around 140 K where the zero σ lattice becomes commensurate.

A transition between two CDW phases, CDW1 at low σ and CDW2 at high σ , where the two phases have very different characteristics, such as E_t and the G anomaly, would explain the weakly first-order length change observed. Such a transition would surely be first order. The presence of a different E_t in the two phases is also natural, as is the different thermopowers. The decrease in the low current R as the transition is approached from the CDW1 side would be due to the lowering of T_p with σ , which would not necessarily be true for CDW2, so that the asymmetry of the transition is natural. The fact that the NBN is nearly the same in both phases is not too disconcerting, especially since the data of Preobrazhensky and Taldenkov¹¹ can be interpreted as showing a $\sim 20\%$ difference in the NBN frequency. It is not so easy to explain the rise in E_t in CDW1 at $T=121$ K and the gradual decrease in the amplitude of the NBN as σ_c is approached. Even if one supposes that the nearness of the transition leads to a fluctuating presence of CDW2, which helps to pin CDW1, why does the same effect not occur in CDW2? Since it is difficult to calculate the pinning potential from first principles, perhaps this puzzle should not be taken too seriously. Thus, we believe that the best explanation for the present data is that there is a transition between two CDW states at σ_c . The monoclinic form of TaS_3 has two transitions, one at 240 and one at 200 K.²¹ These two CDW's may be related in some way to the two CDW's in $o\text{-TaS}_3$ that we propose here, but since the complete structures are not known, we cannot pursue this further.

In summary, we have measured the ϵ - σ relations in o -

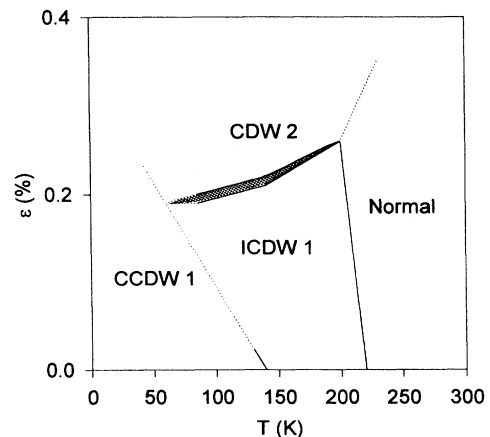


FIG. 7. A possible phase diagram for $o\text{-TaS}_3$, as determined from these experiments and the x-ray data of Wang *et al.* (Ref. 9). The shaded area is a two phase region in which CDW1 and CDW2 coexist. The dotted lines are conjectural.

TaS₃ and found that (1) the change in Y as E increases from 0 to $10E_c$ at 28 Hz is less than 1% and (2) there is an anomaly in the ϵ - σ relations near σ_c , probably due to a weakly first-order transition between two different CDW states. We propose a possible phase diagram for σ -TaS₃ in Fig. 7.

We wish to thank J. McCarten, T.M. Tritt, and J.W. Brill for helpful discussions, and C.W. Schneider for technical assistance. This research was supported in part by the National Science Foundation, Grant No. DMR9312530, and by the Department of Energy, Contract No. DE-FG05-93ER45483.

-
- ¹For a review, see G. Gruner, *Rev. Mod. Phys.* **60**, 1129 (1988).
²T. Sambongi, K. Tsutsumi, Y. Shiozaki, Y. Yamamoto, K. Yamaya, and Y. Abe, *Solid State Commun.* **22**, 729 (1977).
³J. W. Brill, *Solid State Commun.* **41**, 925 (1982); *Mol. Cryst. Liq. Cryst.* **81**, 107 (1982); George Mozurkewich and Ronald L. Jacobsen, *Synth. Met.* **60**, 137 (1993).
⁴J. W. Brill and W. Roark, *Phys. Rev. Lett.* **53**, 846 (1984); J. W. Brill, W. Roark, and G. Minton, *Phys. Rev. B* **33**, 6831 (1986); Ronald L. Jacobsen and George Mozurkewich, *ibid.* **42**, 2778 (1990).
⁵X. -D. Xiang and J. W. Brill, *Phys. Rev. B* **36**, 2969 (1987).
⁶X. -D. Xiang and J. W. Brill, *Phys. Rev. Lett.* **63**, 1853 (1989).
⁷Z. G. Xu and J. W. Brill, *Phys. Rev. B* **45**, 3953 (1992).
⁸K. Tsutsumi, T. Sambongi, S. Kagoshima, and T. Ishigura, *J. Phys. Soc. Jpn.* **44**, 1735 (1978).
⁹Z. Z. Wang, H. Salva, P. Monceau, M. Renard, C. Roucau, R. Ayroles, F. Levy, L. Guemas, and A. Meerschaut, *J. Phys. (Paris) Lett.* **44**, L311 (1983).
¹⁰V. B. Preobrazhensky, A. N. Taldenkov, and I. Yu. Kal'nova, *Pis'ma Zh. Eksp. Teor. Fiz.* **40**, 183 (1984) [*JEPT Lett.* **40**, 944 (1984)]; V. B. Preobrazhensky, A. N. Taldenkov, and S. Yu. Shabanov, *Solid State Commun.* **54**, 399 (1985).
¹¹V. B. Preobrazhensky and A. N. Taldenkov, *Physica B* **143B**, 149 (1986); *Synth. Met.* **29**, F313 (1989).
¹²V. B. Preobrazhensky and A. N. Taldenkov, *Synth. Met.* **29**, F321 (1989).
¹³R. S. Lear, M. J. Skove, E. P. Stillwell, and J. W. Brill, *Phys. Rev. B* **29**, 5656 (1984).
¹⁴T. A. Davis, W. Schaffer, M. J. Skove, and E. P. Stillwell, *Phys. Rev. B* **39**, 10 094 (1989).
¹⁵Z. G. Xu and J. W. Brill, *Phys. Rev. B* **43**, 11 037 (1991).
¹⁶M. J. Skove, T. M. Tritt, A. C. Ehrlich, and H. S. Davis, *Rev. Sci. Instrum.* **62**, 1010 (1991).
¹⁷T. M. Tritt, M. J. Skove, and A. C. Ehrlich, *Phys. Rev. B* **43**, 9972 (1991).
¹⁸D. Maclean, A. Simpson, and M. H. Jericho, *Phys. Rev. B* **46**, 12 117 (1992).
¹⁹W. L. McMillan, *Phys. Rev. B* **14**, 1496 (1976); **16**, 4655 (1977).
²⁰Michael E. Fisher and Daniel S. Fisher, *Phys. Rev. B* **25**, 3192 (1982).
²¹A. Meerschaut, L. Guemas, and J. Rouxel, *C. R. Acad. Sci.* **290**, L215 (1980).